National Physical Laboratory

NPL REPORT MAT 105

UNCERTAINTY OF MEASUREMENT FOR NON-DESTRUCTIVE TESTING (NDT)

M J LODEIRO

MARCH 2022

Department for Business, Energy & Industrial Strategy

FUNDED BY BEIS

UNCERTAINTY OF MEASUREMENT FOR NON-DESTRUCTIVE TESTING (NDT)

M J Lodeiro
Advanced Engineering Materials, Engineering Department

ISSN 1754-2979

DOI: https://doi.org/10.47120/npl.MAT105

National Physical Laboratory
Hampton Road, Teddington, Middlesex, TW11 0LW

This work was funded by the UK Government's Department for Business, Energy and Industrial Strategy (BEIS) through the UK's National Measurement System programmes.

Approved on behalf of NPLML by
Stefanos Giannis - Science Area Leader, Advanced Engineering Materials.

CONTENTS

1 INTRODUCTION

"Uncertainty Evaluation for Non-Destructive Inspection Techniques" (WP4) was part of the Advanced Engineering Materials (AEM) team NMS project on "End-to-End Digitised Materials Testing and Verification" for the advanced manufacturing, engineering, and engineering materials industrial sectors. Within this, activities were proposed to include investigating uncertainty evaluation for non-destructive testing (NDT) inspection techniques.

The activity was devised to consider *up to* two of the NDT methods available at NPL and propose a practical route to uncertainty determination which could then be applicable across other methods by following similar principles. NDT methods are usually performed as relative intensity imaging whether based on optical radiation (laser shearography, thermography), electromagnetics (microwave) or acoustics (ultrasonic c-scan, scanning acoustic microscopy) but there is a lack of uncertainty data as well as deterministic methodologies for quantifying uncertainty of the various parameters which feed into the final image.

This report forms part of the WP4 deliverables summarising the progress towards "A framework for uncertainty determination in Non-Destructive Inspection and digital implementation for one technique."

2 CURRENT INDUSTRIAL PRACTICES FOR UNCERTAINTY DETERMINATION IN NDT

Whilst there is a drive for uncertainties to be considered more broadly in sectors that perhaps historically weren't expected or required to do so, there remains a lot of resistance to the topic, especially in NDT. In particular for bodies to be UKAS (United Kingdom Accreditation Service) accredited or certified as Testing, Inspection or Calibration Laboratories they must comply with internationally recognised quality standards e.g. EN ISO/IEC 17025 [1] which specifically requires information on "uncertainty" to be included in test reports in cases where it affects compliance to a specification limit (see Appendix I for relevant clause). Determining compliance with NDT specifications most often involves assessing whether certain defect types are detected as present or absent, rather than an assessment of numerical test outcomes. However, in cases where numerical compliance criteria apply (such as a minimum allowable thickness or maximum allowable defect size), then the measurement uncertainty (or sizing accuracy) does need to be considered [2].

Part of the reticence to adopt uncertainty in NDT is the cultural change required, but in part this is also related to the nature of NDT instrumentation. Often systems are proprietary, behaving as a black box, where the user has only the most rudimentary awareness of the physical principles and the data processing applied to the output results. In other instances, NDT systems are stand-alone multi-component systems where even something as simple as an A-to-D converter in an ultrasonic c-scan system is integrated into the whole device so verification by accessing relevant ports or dismantling and sending to a calibration laboratory is often impossible. Another consideration is the difficulty for the uninitiated in conceptualizing how uncertainties in signal or position then map across to an uncertainty in a generated image map or even the somewhat creative nature of uncertainty determination which necessarily allows for "guesstimates" of influencing factors and their levels of influence. Frequently the only tangible aspect which operators feel able to control is the output inspection image itself and the process to achieve it (see Section 2.1).

There are nominally two approaches used currently for uncertainty estimation, though not necessarily so widely in NDT: the first is a simplified deterministic approach involving conversion of contributing error ranges to uncertainties (applicable to straightforward measurements) and the second is an empirical approach to uncertainty estimation. The first method involves the following steps:

- List the sources of uncertainty and their error ranges (estimated from experience where necessary),
- Convert each range to a standard uncertainty,
- Combine the contributions from each source, appropriate to the model used to determine the output results from this input data,
- Determine the uncertainty to the appropriate confidence level using the correct coverage factor.

The empirical approach, and potentially a more reliable approach for NDT, can be applied where records on repeated historical measurements on similar parts or results of inter-laboratory comparisons are available already. This approach is suitable provided that the sample size is large enough, where twice the standard deviation of all measurements of a given item, performed by different technicians using different equipment, ideally over an extended time period, would approximate an estimate of uncertainty with a 95% confidence level.

Some worked examples of both routes are available but not widely publicised [3]. As the UK's National Measurement Institute (NMI), the National Physical Laboratory (NPL) necessarily should be involved in assisting with this educational process, leading by example. NPL already has a strong presence in uncertainty training through online and in-person taught courses [4] and the popular Good Practice Guide on uncertainty [5]. To this end, the AEM Group is looking to adopt both these methodologies for the NDT systems available in-house and show others how to perform and record the findings to improve their customer confidence and to ensure compliance with ISO quality standards and UKAS accreditation [6]. From conversations with UKAS assessors and the BINDT (British Institute of Non-Destructive Testing), it is clear that education is required for them also, to enable accreditation bodies to be able to assess compliance, provide advice and simplified guidance to NDT inspection laboratories [7].

Logically, accessing the vast wealth of NPL internal knowledge in uncertainty estimation for complex and varied physical measurement systems is a natural first step. The result of these dialogues is summarised in Section 3, providing a broad framework approach to determining uncertainty for aspects of several NDT systems at NPL.

2.1 IMAGE-BASED UNCERTAINTIES: THE FUTURE?

Ultimately, the ideal would be to devise an uncertainty budget based on repeated measurement of a particular artefact and to use the output images to achieve this estimate. This could comprise multiple historical, consecutive or multiple simultaneous inspections and subsequent statistical analysis of the variability in output. This could then be used to define deviations from an initial check with a specified uncertainty indicating that the system needs maintenance or troubleshooting for problems related to consistent operation or operator error (perhaps requiring more training). More importantly the detailed physics of the interrogating process would be less important, and the methodology could be readily applied across multiple image-generating NDT systems equally. This would potentially remove the need for more in-depth assessment of individual influencing factors which can be challenging since access to fundamental knowledge of sensor function and data processing as the basic input variables for proprietary systems may not be well-understood outside the manufacturer themselves.

There is a strong focus on image analysis and uncertainty in a wide variety of imaging systems within NPL Data Science groups, crossing disciplines and industrial sectors (medical, materials, earth observation, quantum etc). Work on this topic is ongoing and communication with, liaising and input to activities in this area will be maintained throughout the life of the project to ensure any outcomes can be incorporated and specifically targeted for NDT.

3 FRAMEWORK FOR UNCERTAINTY ASSESSMENT OF NDT SYSTEMS

It is good practice for users of NDT systems to test a known artefact before inspection of an unknown part. In practice, this merely provides confidence in the function of the equipment and the operator's ability to image that artefact. Unless the artefact is also representative of the material, geometry and likely defects in the unknown part then there is scope for operator skill or system setup to vary appreciably, diminishing the inspection quality correlation between a reference and customer measurement. This can be mitigated by stringent procedures and operator adherence, but with NDT, much of the expertise is tied up with the individuals performing the measurements. It is rarely the case, especially in the NDT service industry, that the same part design is repeatedly inspected. Even in production environments there is some variety in the nature of the imaged parts, but here it is less impractical to define an inspection procedure to deal specifically with each one, as the finite range of items to be inspected tends to be limited.

This process, whilst limiting errors due to equipment malfunction or operator mistakes, does not provide a quantifiable uncertainty budget for the final results. It is however possible to use a reference artefact to provide quantitative data on the system performance to increase confidence in the results and whilst not providing a calibration, will at least provide some traceability, e.g. c-scan stepped wedge or calibration test blocks.

Reference artefacts are particularly helpful in correlating different systems, new and historical, as technology and data processing changes. Systems are coming on-line now that require daily checks of system performance that qualifies the system before use by running an automated series of inspections of defined reference parts that cover a large volume of the measurement space. These manufacturer-set automated prompts cannot be bypassed and form a continuous record of performance, providing traceability should any results on customer parts be challenged. As manufacturing becomes digital, products will be available with individual data as part of a digital thread with details of the part, system metadata and system telemetry on the measurement or manufacturing device. This thread could also include, for NDT inspection, information on reference artefact results.

Additional to this is the extra layer of error propagation resulting from extracting a measurement from the inspection image (potentially infinite variety of processes), requiring an assessment of the uncertainty in numerical image analysis.

3.1 POSITIONS AND DIMENSIONS

Most inspection systems provide "object maps" providing relative intensity information from location to location over an inspected part, either from a charge-coupled device (CCD) sensor/camera image (such as thermography or laser shearography) or from a point sensor/mechanical scanning bed (microwave, scanning acoustic microscopy or ultrasonic c-scan). In either case, it is possible to assign a correction or uncertainty to the position as defined by the system by using an artefact with features at well-defined locations (this method is used regularly for coordinate measuring machine (CMM) systems at NPL). The object itself can be calibrated for feature location using precision laser or CMM systems and then by

imaging the part with the inspection system and correlating the system response with the known location of the features, either a linear scale correction can be applied or a random statistical variation can be assigned with a normal distribution, allowing the uncertainty in positioning of the system to be defined and hence the uncertainty in the location of any detected defects and their extent within an unknown part. These errors can arise from motion mechanics, dynamic backlash, errors in the system sensors, lens/magnification adjustments or environmental conditions [8, 9].

The issue here is to find an artefact and features which are suitable for the interrogation physics intrinsic to the inspection system. A locating feature with a different thermal response or high optical contrast suitable for a thermal/optical based system is ineffective with ultrasonic systems, and equally a reference that shows good contrast ultrasonically may show no equivalent response in a different system. A series of artefacts (material selection) with different features (ball grids or regions of thermal conductivity contrast or dielectric response contrast) at different length scales optimised specifically to each system will be required. The wide range of NDT systems at NPL makes this a particular challenge as individually designed artefacts are likely to be needed for each. Spherical targets are a good option as the peak position is always at the centre of their location and can be determined by analysing the peak position of returned signal intensity for the inspection system. It also removes issues with identifying the feature “boundary/edge” and therefore locating the centre of planar targets where commonly edge effects result in blurring with signal reduction over a distance equivalent to the sensor beamwidth or the target width, whichever is smaller (where the target is smaller than the sensor beamwidth, the target is perceived to be oversized, approximately the width of the sensor beamwidth).

3.2 ULTRASONIC C-SCAN/SCANNING ACOUSTIC MICROSCOPY (SAM)

Ultrasonic systems interrogate the physical properties of a target by responding to changes in the density and elastic stiffness encountered along the beam path, building up a full map by raster scanning a single point across the surface of a part. SAM operates along the same principles but with a different measurement scale and resolution. Also, many of the factors which influence the ultrasonic time-of-flight contact method will also affect the other ultrasonic systems equally and so these uncertainty assessment processes should be directly transferable (see Section 4.4) with some of the differences highlighted here.

Scanning frames are subject to mechanical vibration and acoustic noise, as well as the electronic noise similarly encountered in contact mode. The c-scan system within AEM has both flatbed 2D scanning, and an additional cylindrical rotation axis as well as a full 3D curve following capability, so the effect of imaging a curved surface with interpolation from a few taught points and the image reconstruction for a cylinder should be considered also (accuracy of angular rotation etc).

Coupling effects for c-scan systems are less significant than for contact ultrasonics as water immersion provides consistent coverage and pressure and defined separations between sensor and target, in this case air entrapment at surfaces may create false positives for near front or back face defects or generate increased uncertainty in background measurements from which the -6dB level is defined for defect sizing. These should be avoided by flushing surfaces with weak detergent wherever possible to improve wetting or otherwise added to the uncertainty budget. The water bath temperature influences the stand-off distance (water velocity sensitive to temperature and timebase delay defines the stand-off position) and potentially the accurate location of the focal plane within the part.

Another difference is that diffraction effects may no longer be ignored, these are material and frequency dependent (being related to wavelength and the size of targets or features within a

target), requiring consideration especially for big stand-off distances and for focussed fields, common in large component c-scanning.

Particular to double through-transmission immersion measurements, where the signal from a support surface behind the part is monitored, the flatness of the support plate can influence the results and should be checked and corrected as far as possible before running an unknown component.

The transducer related uncertainties such as frequency, - 6dB beam width, focal length, filtering etc may all influence the output results and the image quality achieved. Some of these are covered by in-house draft standards but are rarely applied due to a lack of customer demand. Sample effects such as surface finish/losses, curvature, inhomogeneity, perpendicularity of defects to the beam axis etc can influence any numerical dimensional analysis applied to the resulting inspection image.

System acquisition linearity affects the definition of the true -6 or -3 dB width of detected defects as well as the uncertainty in the definition of a reference level from the surrounding material based on which the -6 dB periphery of a defect is taken. For thickness measurements the material homogeneity, nominal ultrasonic velocity and timebase errors will apply.

Liaising with the fundamental ultrasound expertise of the Ultrasonics and Underwater Acoustics (UUA) group at NPL will help to overcome some of the more technically complex aspects of the NDT uncertainty determination and so continued dialogue and assistance are expected going forward.

3.3 ACTIVE THERMOGRAPHY

This system maps the thermal response of a target component subjected to active heating, responding to changes in heat transport through the material. The signal measured by each pixel of a thermal imager is proportional to the intensity emitted by the surface being measured. Spectral intensity is a function of the surface emissivity, wavelength and the temperature of the surface. The emissivity of a surface describes how efficiently that surface can absorb and emit radiation. Emissivity itself is dependent on the wavelength, the temperature, and both polar and azimuthal angles of measurement. When apparent radiance temperatures (emissivity <1) are corrected for an emissivity of 1, they are equivalent to the surface temperature.

The Temperature group at NPL have a system to calibrate thermal cameras which AEM can employ with an associated uncertainty assessment. This looks at uncertainties in the black body used for sensor calibration (considering reference platinum resistance thermometer, emissivity and non-uniformity of target) and the imager (considering size-of-source, non-uniformity in detector, noise, drift, internal reference) [10, 11].

This then leaves primarily the active aspect of NDT thermography to be studied; effect of environment (considering draughts and natural convection, background reflections) and sample (considering heat coverage/intensity using flat black body with Nextel coating, effect of non-uniform emissivity of target, observation angle with respect to the target surface, repeatability, quality of focus etc). Some of these effects can be limited by taking extra precautions during measurement e.g. shrouding to protect against reflections and convection, but these are often not possible in practical applications outside the laboratory environment. For NDT purposes the absolute temperature measured is of less importance than the temperature differential being consistent across all points on the detector, e.g. can ignore atmospheric absorption effect, whilst this changes the absolute temperature observed it does not change the temperature difference as the absorption will be consistent across the part, but

the calibration process described can be modified for NDT purposes.

3.4 LASER SHEAROGRAPHY

This system maps changes in the out-of-plane displacement gradient of a surface when subjected to applied stress (heat, pressure, load etc) relative to an initial reference condition, responding to changes in surface deformation. This is essentially a form of laser speckle interferometry but with some compensation for vibration sensitivity which these systems often suffer from within industrial settings. Each pixel has a defined phase change caused by deformation ($\pm n\pi$) which is associated with a distance based on the illuminating wavelength. This is a particularly complex system to provide uncertainty budgets for due to the nature of the optical and phase data manipulation, and also considering that the strength of this technique is its almost infinite accommodation of different NDT situations: scaling up or down in area measurement, varying resolution, lenses/magnification, defect sensitivity etc. The orientation of the camera to the part, uneven heating, draughts, quality of focus, shear angle and shear offset etc can all impact the output but in ways which may be difficult to define. This method would require a period of focused investigation to assess the root cause and influence of all likely contributing factors. As such this method has been covered only briefly by this initial work package.

Spatial correlation can be performed as described earlier with an appropriate reference (see Section 3.1). This system has automated intrinsic conversion to engineering units with a pair of class 1 laser pointers at a fixed separation on the camera body targeted on the inspected surface and the known distance versus pixel count calculation provides the image scaling. However, this defines the scaling at two points at the centre of the sheared image but does not define any equivalence elsewhere in the image-field, accounting for any possible lens distortion or corrections, so this also needs to be considered.

3.5 MICROWAVE

This system monitors the amplitude of the standing wave generated between the injected microwave signal and the multiple reflected waves from the inspected part, responding to the dielectric properties in the beam path, building up a map by raster scanning across the part. This standing wave is sampled within the sensor head at positions separated by a quarter wavelength to minimise the risk of a single detector being coincidentally placed at a standing wave node which might otherwise return an all-null dataset with no structural contrast. The detector does not record the maximum signal nor is there any time separation nor any amplitude reference between returned compared to injected microwaves. Spatial correlation can be performed as described earlier with an appropriate reference (see Section 3.1).

The ideal solution for the signal response gain, linearity, stability, offset, noise and resolution would be to inject a known signal with traceable calibrated origins and monitor the effects on the acquired data for each channel. The sample effects would then need to be taken into account e.g. surface roughness, orientation, surface proximity (affecting phase of return signal and superposition with injected beam) and any environmental factors e.g. EM noise, stray pickup from nearby dielectric objects, background effects etc.

It is not yet known if this is strictly possible for microwaves (requires discussions with experts in the Electromagnetic Measurements field within NPL). Alternatively, a common approach for other dielectric measurements involves calibrating against reference material responses. More targeted research into this may be required before a complete solution can be prescribed for uncertainty determination.

3.6 UNIQUE INFLUENCE FACTORS

It is recommended to study the effects of metrological characteristics of the inspection system separately from the effects of the sensor-sample interaction, e.g. material effects or probe behaviour, wherever possible since sensors and inspected parts can change frequently and if measured in unison the uncertainty in the underlying system would need to be revisited every time [9].

Other metrological characteristics of inspections which aren't applicable across all systems could also potentially be investigated with reference artefacts, e.g. the effects of roughness, flatness, thickness, reflectivity/emissivity, camera distortion or resolvability on the output uncertainty, providing a route to additional calibration standards or providing evidence of the need to control the unique influencing factors for each NDT system.

4 UNCERTAINTY BUDGET EVALUATION FOR TIME-OF-FLIGHT MEASUREMENTS

Most NDT inspection techniques provide images for assessor analysis and do not readily lend themselves to uncertainty budgets for the constructed image map, though uncertainty budgets can be determined and applied to individual aspects of the contributing data (e.g. position, timing or signal amplitude). However, determining a model which enables all of these contributions to be combined in a way which is representative of the uncertainty in the whole image is not trivial. Ultimately this base level verification can only provide confidence in the functioning of the NDT system, since defects and materials all behave differently under even a single form of interrogation, one cannot extrapolate the successful system operation with successful defect detection. This requires a lengthy and labour-intensive programme of a statistically significant number of measurements to determine a probability of detection (PoD) distribution, taking into account detectability of the desired defects within a specific material/geometry at different length scales as well as operator variability.

As an initial look at NDT uncertainty budget determination, the time-of-flight method of ultrasonic material velocity measurement was selected. This method, available as part of the suite of NDT consultancy measurements available in AEM, generates a numerical output and as such is more readily assessed for uncertainty and can be expressed in a traditional manner.

4.1 BACKGROUND

Ultrasonic velocity can be derived using either pulse-echo or through-transmission techniques, with transducer coupling being provided by direct transducer contact or indirectly through water immersion. Immersion is particularly useful when the material tested is soft and the use of direct contact testing could deform the surface where probes are pressed with sufficient force to provide suitable acoustic coupling. Sharp, transient pulse transit methods are employed, assuming the first acoustic arrival propagates along the shortest path at the bulk velocity, i.e. as though in an infinite medium, which is true provided the wavelength is less than one-fifth of the solid specimen's lateral dimensions along the path of wave propagation. Lateral dimensions of the sample should be adequate to ensure no interference of edge effects and sample thickness should avoid interfering echoes if too thin or excessive attenuation if too thick.

For many materials, acoustic velocity can span a range of values due to material processing variations as well as the mechanical and acoustic measurement tolerances. Solids may be inhomogeneous and anisotropic such that actual values depend on exact composition, orientation, temperature, frequency, measurement method and pressure or stress (see Appendix II for evidence). Some of these are considered in more detail here.

Immersion measurements of characteristic longitudinal ultrasonic material velocity have been available as an NPL Measurement Service for many years within UUA. However, on occasion, customers require both longitudinal and shear velocities to enable the material to be modelled more fully in the acoustic regime or for full elastic property determination of small material volumes. Shear waves do not propagate in fluids (liquids, gases) where shear polarisation is dissipated and undefined. Whilst shear velocity determination is still possible with immersion methods (by rotating the sample to create non-normal beam incidence and monitoring the location and path length of the mode converted quasi-shear and quasi-longitudinal waves), it requires extensive re-engineering of current systems to allow for precision-controlled sample rotation on-axis within the beam, suitable sample clamping and mathematical modelling to enable a fitting of multiple off-axis measurements to define the best shear velocity from the calculated off-axis refracted path lengths. There is the added complication of anisotropic materials displaying different shear velocities in different propagation and polarisation material planes which must also be accommodated experimentally.

This process is simpler where transducer crystals are available cut in x- (compression wave) or y- (shear wave) axes and direct contact between the crystal and the interrogated material surface (using a suitable gel or molasses couplant) enables both wave modes to propagate in the material along a well-defined propagation and polarisation path. As a result, since both contact transducer types are readily available as part of the routine assessments carried out for CR&D work within the AEM NDT group, this velocity determination method is now regularly applied for customer work where both velocities of longitudinal and shear wave types are required. An assessment of the measurement uncertainty for the determination of these velocities is therefore essential.

4.2 MEASUREMENTS

Before testing, sample thicknesses are measured using a micrometer. Specimens are allowed to equilibrate to the local temperature for 24 hours before testing and are handled using insulating gloves to minimise any variable temperature effects on either the sample thickness or subsequent pulse timing measurements. Thickness measurements are made at a minimum of 5 separate positions covering the whole sample area.

The ultrasonic velocity measurements are carried out in through-transmission contact using the rig shown in Figure 1. This controls the probe alignment and provides a controlled pressure on the probes generating a consistently thin couplant layer. In this configuration, the single transit path from transmitter (Tx) to receiver (Rx) limits the attenuation and scatter losses compared to the pulse-echo double transit path (and corresponding multiple repeat echoes) method (though the pulse-echo method can also be performed where preferred or where samples are too thin to sensibly measure a single transit delay time). A distinct timing feature is used to define the arrival time of the signal. The nearer to the first arrival that the feature is chosen, the less significant are the various end effects and unwanted boundary reflections (though it should be noted this timing method performs poorly for materials that have frequency dispersion or high losses). In this case, the zero crossover between the principal positive and negative going peaks of the broadband pulse are used, as this is less ambiguous than the signal start, but still occurs sufficiently early in the pulse waveform to limit any errors of waveform distortion caused by dispersion (frequency dependent velocity), scattering and frequency dependent attenuation.

Initially, reference measurements are made with the transducers in direct contact with each other. There is a finite time required for the signal to travel from the point of excitation (piezoelectric crystal) after triggering, through the transducer wear-plates, couplant, the receiver transducer and processing electronics, and then be evaluated by the acquisition

software. Measuring the 'zero sample thickness' transit time accommodates for this fixed offset time to derive a more accurate 'sample only' transit time. Similarly, this reference measurement captures the effect of the load and temperature on the transducers and electronics performance, and the contribution of the couplant layers to the transit time which, as these parameters are thus controlled to be approximately constant throughout the testing process, minimises their unwanted effects on the final data. The load applied between the probes is maintained at ~20 N, with and without samples in place, monitored using an in-line load cell and displayed on an RDP E308 indicator. The load is captured simultaneously with the time-of-flight data. The temperature of the samples is monitored with a PRT sensor using a thermal interface sheet to improve thermal contact with the solid surface and displayed on an accurate temperature acquisition device. The ambient room temperature is also monitored to check for significant deviations during testing.

With the probes aligned and in contact, the ultrasonic system is used to tune the pulser and receiver to the appropriate settings, monitoring for signal amplitude and distortion/saturation issues. The receiver filtering is adjusted for high and low pass filtering as required and the gain adjusted to produce a non-saturating RF signal on the A-scan display suitable for both reference and sample signals.

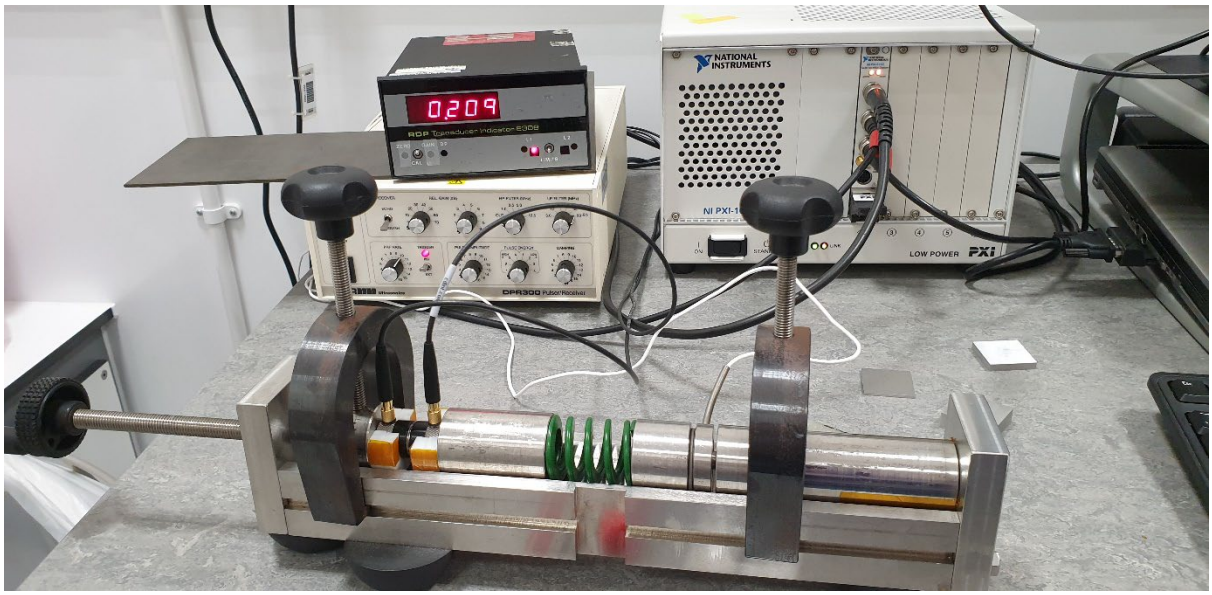

Figure 1 Ultrasonic time-of-flight measurement rig.

When a sample is placed between the Tx and Rx probes in the signal path, the A-scan signal is observed to shift in time and the peak signal amplitude decreases. The system is allowed to stabilise under load before measurements are acquired. The received echoes are kept below 500 mV with a consistent gain setting throughout to avoid non-linearity in the receiver/amplifier response affecting the arrival times.

The ultrasonic velocity *v*, either shear (*s*) or longitudinal (*l*), for single transit contact measurements is given by:

$$v_{s,l} = \frac{d}{\Delta t_{s,l}}$$

Where *d* is the propagation distance (sample thickness in this case) and Δt is the time of flight of the pulse through the material (in this case the time measured for the sample correcting for the reference time with no sample in place).

Signals are digitised and captured using a 14-bit high speed digitiser. The digitiser captures at 100 MS/s but to achieve the 1 ns timing resolution required, random interleaved sampling of 10 consecutive acquired signals is employed. These are averaged over 25 full repeated waveforms to generate a single waveform for analysis. The maximum and minimum of each waveform is found, and a polynomial is fitted to all the waveform data between those points. The zero crossover from the best fit is then determined and captured. This is repeated 'live' for multiple consecutive pulse repetitions (>200) and a Gaussian distribution fitted to the cumulative results. The peak and standard deviation of this fit is then captured to provide the transit time for each sample measurement.

Whilst velocities can be calculated in this way for a single sample with a known thickness, an improved estimate can be achieved by repeating for several samples of different thicknesses and finding the best fit line to the extended data. In this way the reference measurement does not need to be subtracted from each sample time-of-flight but rather forms the time-of-flight for zero sample thickness. This multiple thickness measurement also highlights any deviations from linearity (indicating measurement problems or dispersive material) which would invalidate the underlying measurement assumptions. This process is performed multiple times for each sample thickness (between 3 and 10). For isotropic materials (see Section 4.3 for more details), each measurement repeat requires removal and replacement of the sample within the fixture with a quarter turn rotation, and the reapplication of the same load.

This procedure is duplicated for all the different sample thicknesses available, with both compression and shear probe pairs. Once all the transit times are determined, the average specimen thickness and individual arrival time data are plotted and a straight line fitted to all the datapoints to determine the characteristic material velocities at the stated ultrasonic frequency of measurement.

4.3 SPECIMEN SYMMETRY/PREPARATION

Multiple samples are required, each with different thickness but all with the thickness direction (propagation path) identically oriented along a defined material axis of symmetry. The propagation contact specimen faces must be as flat and parallel as possible to limit the uncertainty associated with the thickness and transit time measurements due to the specimen.

If the material is fully isotropic, measurements along any axis are identical and no special considerations of sample orientation are necessary. If the material is nominally transversely isotropic, then all but one of the symmetry axes are identical and the principal axis should be defined along the thickness. This ensures no special considerations of sample orientation between the transducers, only the propagation axis must be considered. In cases where the material is orthotropic (due to rolling, hammering etc), all 3 orthogonal material axes are different, and each sample edge must be marked with the relevant alignment axis to allow precise definition of the propagation direction (for shear and compression wave) and polarisation directions (for shear wave). In this case, compression and shear velocities may be different in different directions and the elastic compliance matrix defines the number of independent velocities which characterise the material (determination of all of these may require off-axis samples cut at defined angles to the main symmetry axes). In particular, shear wave propagation occurs within a plane and shear velocities could accordingly be different for transit along the same propagation path but oriented with different polarisation axes.

4.4 UNCERTAINTY METHODOLOGY

Firstly, an assessment of the direct and indirect sources of uncertainty contributing to the measurement process was carried out, summarised in Table 1. Direct sources are those that contribute directly to the measurement of either thickness or time from which the velocity is then calculated. Indirect sources are those which affect the measured result in uncontrolled or ill-defined ways, e.g. frequency, temperature or load.

A summary of the test equipment used in the assessment, and the calibration details where appropriate, are given below.

- Sample thicknesses measured using Mitutoyu 0-1” MDC – 1” MX digimatic micrometer, Serial No. 67470071, Cert. No. 317736 calibrated to ± 0.002 mm (metric equivalent) expanded uncertainty at 95% confidence with a coverage factor k=2.
- Transducer excitation and received signal conditioning using JSR Ultrasonics DPR300 pulser/receiver.
- Contact probes used were Panametrics V110 longitudinal and V156 shear transducer pairs. These have a 6 mm diameter and nominal 5 MHz centre frequency.
- Signal acquisition using National Instruments PCX 5122 14-bit high speed digitiser 100 MS/s housed in a PXI 1033 chassis with LabView software control and data capture.
- Applied in-line load monitored using an RDP Electronics model 53 miniature 2.2 kN compression load cell with an E308 amplifier and indicator, verified with a calibrated Instron load cell Serial No. 2580-1kN/138012, Cert. No. E265080521131121 calibrated to ± 0.38 N expanded uncertainty at 95% confidence with a coverage factor k=2 for 0-200 N range in compression.
- Sample and ambient temperature monitored using PRT 10 ITS 90 4 wire temperature sensor with Fluke 1586a super daq precision temperature scanner with resolution 0.005 K (0.2 °C uncertainty for coverage factor k=1 assumed when not calibrated in conjunction with sensor).

It is interesting to note that there can be significant differences between published values for acoustic velocities of the same named material. An example of this variability is shown in Table 2 for aluminium and some of its alloys, also of interest is the omission of any associated uncertainties quoted with the reported values. Metals can have significant variation in acoustic properties due to rolling effects on grain structure, heat treatment and/or residual stresses [12]. As a result of their processing, some materials can be anisotropic with respect to velocity. Similarly, polymers can have acoustic variation due to their processing as well. Some are extruded while others are cast, formulation changes, crystallinity etc. Unlike metals with well-defined alloy compositions, polymers can also have minor differences in formulation for materials of the same name depending on the manufacturer.

Table 1 Sources of uncertainty in time-of-flight measurements

Uncertainty source	Comments
Temperature	• Affects transducer performance and changes sample dimensions (aluminium and alloys CTE ~13x10^{-6}/°C so 10 °C change results in ~1.3 μm length change or 0.2 ns change for longitudinal wave ToF) • Speed of sound in material intrinsically increases with temperature • Unknown effect on hardware so ambient temperature controlled • Reference measurements at zero thickness effectively accommodate intrinsic temperature effects on measurement probes/electronics
Frequency	• Higher frequencies are generally attenuated more quickly than lower frequencies which may cause changes to the broadband pulse waveform shape affecting the relative time location of timing features • Possible selective attenuation caused by grain size distribution and phase segregation in metals/ceramics • Dispersive viscoelastic materials (polymers) will show large changes with frequency • Sharpness of timing transition etc affected by frequency, through timing and amplitude resolutions • Non-linearity of amplifiers with frequency
Load	• For contact measurements only • Affects transducer response, sample stress/dimensions/velocity • Affects couplant layer thickness • May affect sample thickness for soft materials – keep as low as possible to maintain good acoustic contact • Load cell in-line and load controlled manually to within 1 N of nominal value for all measurements • Load cell corroborated against calibrated load cell
Sample thickness	• Accurate to measuring device calibration/resolution • Additional errors may be present due to non-parallel machining of sample contact faces • Multiple measurements (minimum 5) over sample surface • Care to estimate a true thickness when the material is soft such that contact with the calliper or micrometer causes it to compress
Timing accuracy/stability	• Timing based on digitiser timebase i.e. 1GS/s usually applied for this work • Jitter in receive electronics or triggering potentially a larger effect for timing • Some correction by removing timing delay in signal travelling through circuits and transducers themselves on zero thickness reference measurement with repeatable couplant thickness • Interleaving multiple signals into a single waveform incorporates jitter and trigger deviations into each timing measurement
System gain/stability/ amplitude resolution (14-bit)	• Linearity of amplifier response with frequency • Signals kept below 500 mV and gain maintained constant throughout all measurements • Electronics jitter • Noise floor changes due to gain levels • Bit depth effect with high gains
Diffraction	• Correction required for focussed fields or long path lengths in immersion measurements • Not significant here due to near-field measurements, small distances and plane piston transducers • Probes located away from sample edges
Couplant	• Uniformity across the sample surface • Consistency between different samples • Some correction by removing timing delay in signal travelling through couplant on zero thickness reference measurement • Some control on layer thickness by applying same in-line load with every measurement

Table 2 Comparison of reported acoustic velocity values for aluminium and its alloys

Source	Material	v_l (m/s)	v_s (m/s)
Engineering Toolbox https://www.engineeringtoolbox.com/sound-speed-solids-d_713.html	aluminium	6420	3090
Olympus https://www.olympus-ims.com/en/ndt-tutorials/thickness-gauge/appendices-velocities/	aluminium	6320	-
Dakota Ultrasonics https://dakotaultrasonics.com/reference/	aluminium	6375	3130
Pan American Industries https://www.panamiris.com/downloads/UltrasoundVelocity.pdf	250	6350	-
	2024	6405.88	-
	17ST	6238.24	-
Class Instrumentation https://www.classltd.com/sound-velocity-table/	aluminium	6300	-
Onda https://www.ondacorp.com/wp-content/uploads/2020/09/Solids.pdf	aluminium (rolled)	6420	3040
	6262-T9	6380	-
Guanyu Tube https://tubingchina.com/Ultrasonic-Velocity-Acoustical-Properties-Of-Common-Materials.htm	1100-0	6229	3073
	2024-T4	6375	3150
	6061-T6	6299	3150

4.4.1 Uncertainty Budget

Despite the deceptive simplicity of the measurement process, inputs and calculations; the uncertainty estimation is actually more complex than covered by most standard statistical texts. Each specimen thickness generates its own sample population of both thickness and time-of-flight and these can vary for each specimen over the range of thicknesses used. Combining these individual sample population data with the linear fit process is also beyond the average statistical text. For simplicity, these are considered separately: the input parameter uncertainties and the linear fit uncertainty applied to all the measurement datapoints. Discussions are underway with NPL Data Science group to find a means of combining all the uncertainties into one inclusive value. In the meantime, the worst case of the individual uncertainties for thickness and time-of-flight are used to define the error bars across all individual points (useful in data plots) and the linear fit analysis is used to define the uncertainty in the velocity measurement using the slope of the fit, ignoring the individual uncertainty contributions of thickness and time-of-flight in this case.

Table 3 Uncertainty determination of input data for ultrasonic velocity determination calculated for each specimen thickness/time of flight sample population with N measurements of each

Sources of Uncertainty					Uncertainties				
Name	**Measurand**	**Type**	**Value**	**Source**	**Probability Distribution**	**Divisor**	**Standard Uncertainty**	**Sensitivity Coefficient**	**Degrees of Freedom**
Micrometer calibration	Transit path	B	0.002032	Calibration certificate	normal	2	0.001	1	∞
Micrometer resolution	Transit path	B	0.0005	Micrometer	rectangular	√3	0.00029	1	∞
Measured thickness	Transit path	A	σ (*d*)	Specimen	normal	1	σ (*d*)	1	N-1
units	mm								
Timing calibration	Transit time	B	-	n/a	normal	-	-	1	∞
Timing resolution	Transit time	B	0.5	5122 digitiser	rectangular	√3	0.29	1	∞
Measured times	Transit time	A	σ (*t*)	Specimen	normal	1	σ (*t*)	1	N-1
units	ns								
***Linear fit**	*currently treated separately								

NB: The timing calibration is currently unknown. This needs to be verified in conjunction with the data acquisition system and checked with a high precision calibrated oscilloscope. This is still being investigated to determine the best route. It is likely to have a very small impact on the overall uncertainty and so work on the uncertainty framework was continued despite this omission.

In general, the low number of repeat measurements per specimen (necessary due to the time required for a set of measurements being prohibitively long otherwise) gives a lower sample population than is appropriate for fitting to a normal distribution and so the use of a student t-distribution will ordinarily provide a better representation in practice [5]. If we assume we have 3 different specimen thicknesses (subscript 1,2,3), the standard uncertainty due to the specimen is calculated by:

$$u_1(d)=\sigma_1(d)/\sqrt{N_1}$$
$$u_2(d)=\sigma_2(d)/\sqrt{N_2}$$
$$u_3(d)=\sigma_3(d)/\sqrt{N_3}$$

The largest of these is then taken as the specimen uncertainty of thickness across all samples and used for the combined uncertainty budget for thickness. A similar process is then applied to the time-of flight data captured for each specimen thickness.

The standard uncertainties for each separate contribution to the overall thickness or time-of-flight uncertainties are determined by (data extracted from Table 3):

$$u_{cal,\ res,\ spec}=\text{‘value’/‘divisor’}$$

The combined uncertainty can then be found by adding the contributions in quadrature, calculated as:

$$u_c(d)=\sqrt{[(u_{cal})^2+(u_{res})^2+(u_{spec})^2]}$$

and similarly for $u_c(t)$. In line with the process for determining the coverage factor for t-distributions, using the Welch-Satterthwaite equation [13], the effective degrees of freedom, ν_{eff}, for the thickness and time-of-flight are determined from their respective contributions (ignoring contributions which have infinite degrees of freedom as these are vanishingly small and the effect of sensitivity coefficients as these are all 1 in this case) as:

$$\nu_{eff}\,(d)= (u_c(d))^4/[(u_{spec}(d))^4/\nu_{spec}]$$

and similarly for $\nu_{eff}\,(t)$. These effective degrees of freedom define the shape of the t-distribution for each measurand and most importantly define the coverage factor k to provide a 95% confidence interval. For normal distributions this is 1.96 (usually rounded to 2) but for t-distributions the 95% coverage factor can be found from tables (interpolation may be required to give the best interval for the target ν_{eff}).

This is then used to provide the expanded uncertainty for each of the measurands, thickness and timing, by:

$$U_{expanded}(d,\,t)=k_{d,\,t}\,u_c(d,\,t)$$

These expanded uncertainties are used to define the error bars on the data plot from which the linear fit is determined as shown in Figure 2.

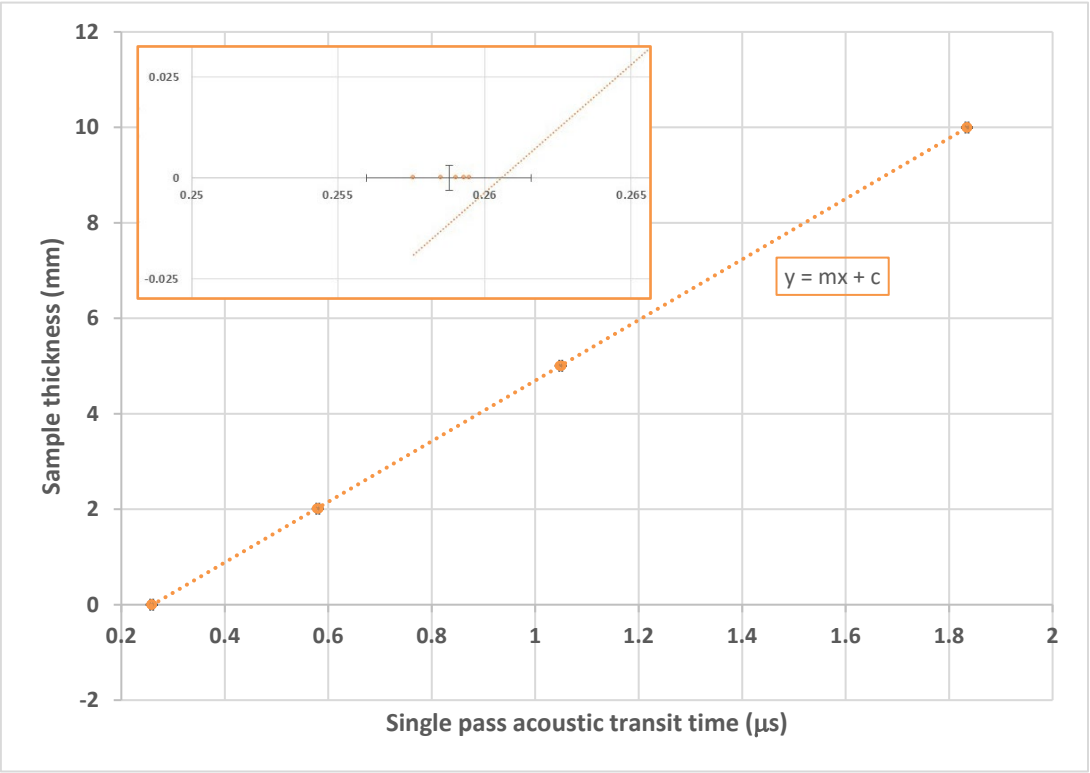

Figure 2 Typical plot of thickness/time-of-flight data for set of specimens and reference measurements using ultrasonic waves in contact mode. Expanded region inset shows thickness and time-of-flight uncertainties (3.1 µm and 2.8 ns in this case to 95% probability) to provide confidence in the data populations for each specimen thickness.

The uncertainty associated with the linear fit and applied to the velocity calculation treats the repeatability (effectively the "noise" in the data) as the only source of uncertainty ignoring the contributions of uncertainty from the time or thickness determined earlier. Suppose we have a set of measurements of a control quantity *X* and a response quantity *Y*, and that we want to fit a function *f(X, α)* where *α* is a set of *M* parameters. Then we seek to minimise:

$$\sum_{i=1}^{N}(f(x_i,\alpha)-y_i)^2=\sum_{i=1}^{N}r_i^2$$

If the uncertainties associated with *x* can be neglected, then the covariance matrix associated with the parameters *α* is given by:

$$V=\hat{\sigma}^2(J^TJ)^{-1} \qquad \text{where} \qquad \hat{\sigma}^2=\frac{1}{N-M}\sum_{i=1}^{N}r_i^2$$

is the sum of squares of the residuals evaluated at the best fit values of *α* and *J* is the *N* by *M* Jacobian matrix whose (*i*, *j*) entry is given by:

$$J_{ij}=\left.\frac{\partial f}{\partial \alpha_j}\right|_{x=x_i}$$

For a straight line fit, we get:

$$\sum_{i=1}^{N}(mx_i+c-y_i)^2=\sum_{i=1}^{N}r_i^2$$

so that the Jacobian matrix is:

$$J^TJ=\begin{bmatrix}\sum x_i^2 & \sum x_i\\ \sum x_i & N\end{bmatrix} \qquad \text{where} \qquad J_{i1}=x_i,\quad J_{i2}=1,\quad i=1,2,\ldots,N$$

and its inverse is:

$$(J^TJ)^{-1}=\frac{1}{N\sum x_i^2-(\sum x_i)^2}\begin{bmatrix}N & -\sum x_i\\ -\sum x_i & \sum x_i^2\end{bmatrix}$$

A best fit line has two parameters, so that:

$$\hat{\sigma}^2=\frac{1}{N-2}\sum_{i=1}^{N}r_i^2$$

and hence:

$$u_m^2=\frac{N\frac{1}{N-2}\sum_{i=1}^{N}r_i^2}{N\sum x_i^2-(\sum x_i)^2} \qquad \text{or by rewriting} \qquad u_m^2=\frac{\frac{1}{N-2}\sum_{i=1}^{N}r_i^2}{\sum x_i^2-\frac{1}{N}(\sum x_i)^2}$$

In summary, to calculate the uncertainty associated with the slope of the best fit line:

- Fit the line to all the datapoints to find m and c
- Calculate the residuals $r_i = y_i - mx_i - c$
- Calculate $\sigma^{\wedge 2}$ as above
- Calculate u_m^2 as above and take the square root to get the standard uncertainty u_m.

This applies where both slope and intercept are allowed to vary freely in the fitting process. A small modification is required where the intercept is fixed to pass through a particular value, e.g. the origin.

The next step is to determine the best route to combine the uncertainty analyses so that individual contributions and the global fit are encompassed into a single quantity.

5 SUMMARY AND RECOMMENDATIONS

This work has provided a perspective on the current practices in uncertainty estimation in the NDT industry and, through collaboration with experts in their fields within NPL, a broad methodology to begin to establish the uncertainty budgets for the NDT systems within AEM.

We have improved our connections with RCNDE, BINDT and UKAS to continue to advance this topic more broadly in the industry, in readiness for Industry 4.0 and improved traceability, and also to ensure the activities within NPL remain relevant and do not become academic exercises with little utility outside a dedicated NMI laboratory.

In particular, detailed assessments of the uncertainty contributions within ultrasonic time-of-flight/velocity measurements have been performed, highlighting some omissions in knowledge and understanding which can be addressed in the short term. This work feeds also directly into the ultrasonic c-scan work proposed for study next year, advancement in the ToF uncertainty determination advances the c-scan uncertainty determination, particularly timebase uncertainty and amplitude stability/gain linearity measurements which are also the fundamental measurements required to generate c-scan images. Inter-department activities between AEM NDT and UUA are expected to continue on this topic.

The determination of timebase accuracy has long been a problem in multiple measurement systems within AEM with no obvious route forward. After discussions with experts in other areas of NPL it seems that timebase traceability should be possible and this knowledge could benefit both the ToF and ultrasonic c-scan NDT system but also other acoustic measurement systems more broadly, e.g. impact excitation. Also the error combination required to provide a complete uncertainty solution for the time-of-flight measurement process will be discussed further with colleagues in Data Science (shortly after publication) to ascertain if a complete integrated solution is possible. This would add understanding which can be shared with others dealing with similar seemingly simple but non-trivial data processes.

The approach in the following year would be to look at both baseline measurements (deterministic uncertainty) and also repeatability work (empirical approach) as far as possible to assess the uncertainty in defect detection and sizing for flat and curved parts and thickness mapping for ultrasonic scanning systems and for factors influencing active thermography.

It is planned to remain engaged with the image uncertainty activities within Data Science in the next NMS period to extract as much value and provide as much direction to the benefit of NDT as possible, in the hope of an alternative or additional route to uncertainty assessment for NDT inspections in the future.

6 REFERENCES

[1] ISO, *ISO/IEC 17025:2017 General requirements for the competence of testing and calibration laboratories,* 2017.

[2] National Association of Testing Authorities (NATA), “Measurement Uncertainty,” Australia, Feb 2010.

[3] National Association of Testing Authorities (NATA), “Measurement Uncertainty in Non-destructive Testing (Worked Examples in: Magnetic Particle, Ultrasonic Thickness, Penetrant Testing),” Australia, 2010.

[4] National Physical Laboratory, “NPL e-learning courses,” 2019. [Online]. Available: https://training.npl.co.uk/sector/e-learning-courses/.

[5] S. Bell, “The Beginner's Guide to Uncertainty of Measurement, Good Practice Guide No. 11,” National Physical Laboratory, UK, 1999.

[6] European Accreditation, *EA-4/15 G:2015 Accreditation for Non-Destructive Testing (withdrawn),* 2015.

[7] National Association of Testing Authorities (NATA), “Non-destructive Testing ISO/IEC 17025 Application Document,” Australia, 2013.

[8] Z. Qiang and W. Wei, “Calibration of laser scanning system based on a 2D ball plate,” *Measurement,* vol. 42, no. 6, pp. 963-968, July 2009.

[9] C. L. Giusca and R. K. Leach, “Calibration of the metrological characteristics of Coherence Scanning Interferometers (CSI) and Phase Shifting Interferometers (PSI), Good Practice Guide No.127,” National Physcial Laboratory, UK, 2013.

[10] J. L. McMillan, A. Whittam, M. Rokosz and R. C. Simpson, “Towards quantitative small-scale thermal imaging,” *Measurement,* vol. 117, pp. 429-434, 2018.

[11] J. L. McMillan, A. Greene, W. Bond, M. Hayes, R. Simpson, G. Sutton, G. Machin, J. Jowsey and A. Adamska, “Thermometry of intermediate level waste containers using phosphor thermometry and thermal imaging,” *Measurement,* vol. 132, pp. 207-212, 2019.

[12] E. Ginzel and B. Turnbull, “e-Journal of Nondestructive Testing 2016-12,” 2016. [Online]. Available: https://www.ndt.net/article/ndtnet/2016/17_Ginzel.pdf.

[13] K. Birch, “Estimating Uncertainties in Testing, Good Practice Guide No. 36,” British Measurement and Testing Association, 2001.

7 APPENDIX I

The relevant clause quoted from ISO/IEC 17025:2017 is:

7.6 Evaluation of measurement uncertainty

7.6.1 Laboratories shall identify the contributions to measurement uncertainty. When evaluating measurement uncertainty, all contributions that are of significance, including those arising from sampling, shall be taken into account using appropriate methods of analysis.

7.6.2 A laboratory performing calibrations, including of its own equipment, shall evaluate the measurement uncertainty for all calibrations.

7.6.3 A laboratory performing testing shall evaluate measurement uncertainty. Where the test method precludes rigorous evaluation of measurement uncertainty, an estimation shall be made based on an understanding of the theoretical principles or practical experience of the performance of the method.

NOTE 1 In those cases where a well-recognized test method specifies limits to the values of the major sources of measurement uncertainty and specifies the form of presentation of the calculated results, the laboratory is considered to have satisfied 7.6.3 by following the test method and reporting instructions.

NOTE 2 For a particular method where the measurement uncertainty of the results has been established and verified, there is no need to evaluate measurement uncertainty for each result if the laboratory can demonstrate that the identified critical influencing factors are under control.

NOTE 3 For further information, see ISO/IEC Guide 98-3, ISO 21748 and the ISO 5725 series.

8 APPENDIX II

Effects of load/pressure and frequency on acoustic velocity measurement in practice are shown in the ultrasonic velocity data plots below.

Measurements were made on a single set of 3 specimens using transducers with pulsed excitation and broadband performance: 5 MHz 6 mm diameter, 5 MHz 12.5 mm diameter and 1 MHz 12.5 mm diameter probe pairs. Apart from the c_2 value being significantly different from c_1 and c (expected due to the waveform width difference between 1 and 5 MHz nominal centre frequencies); there is < 0.5 % change between m_1 and m, i.e. different probe areas at the same frequency, roughly associated with applied pressure (load the same in both cases but applied sample pressure for larger transducers reduced to ¼ compared to smaller transducers) and there is < 1.5 % change between m_1 and m_2, i.e. different probe frequencies at the same diameters (load and hence applied sample pressure the same in both cases).

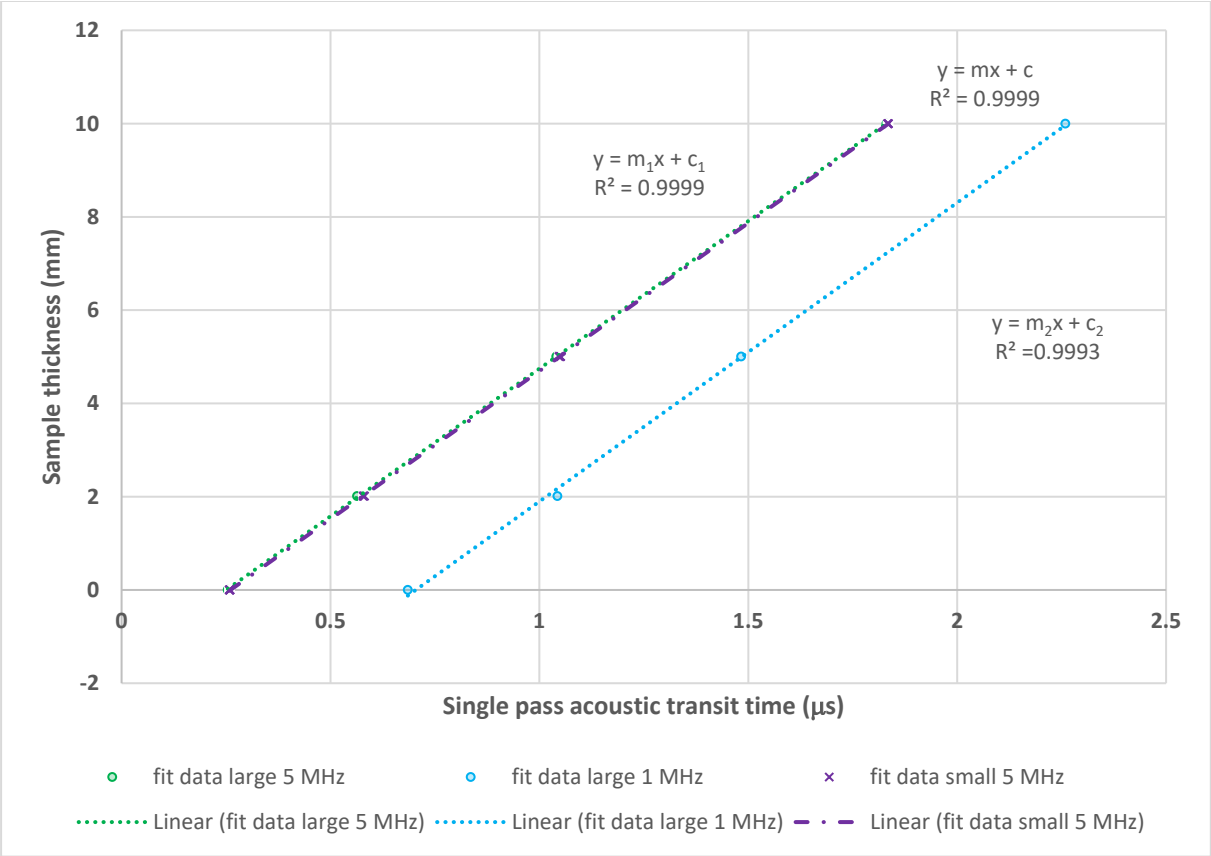

Figure A1 Typical plot of thickness/time-of-flight data for set of specimens and reference measurements using ultrasonic waves in contact mode with different frequency and diameter probes.